Journal of the European Ceramic Society 22 (2002) 2939–2944

www.elsevier.com/locate/jeurceramsoc

Crystalline structure and electrical properties of $YCu_xMn_{1-x}O_3$ solid solutions

D. Gutiérrez[a], O. Peña[b], P. Durän[a], C. Moure[a,*]

[a]*Instituto de Cerámica y Vidrio, CSIC, Departamento de Electrocerámica, 28500 Arganda, Madrid, Spain*
[b]*Chimie du Solide et Inorganique Moléculaire (CSIM), UMR-CNRS 6511 Université de Rennes Cedex, France*

Received 4 July 2001; received in revised form 11 February 2002; accepted 24 February 2002

Abstract

Solid solutions belonging to the Mn-rich region of the $YCu_xMn_{1-x}O_3$ system have been studied. The powders were prepared by solid-state reaction between the corresponding oxides. Sintered ceramics were obtained by firing at 1100–1325 °C. The incorporation of 30 at.% Cu to the yttrium manganite induces the formation of a perovskite-type phase, with orthorhombic symmetry. Increase of the Cu amount do not appreciably affects the orthorhombicity factor b/a, up to an amount of 50 at.% Cu. Above this Cu amount, a multiphase system has been observed, with the presence of unreacted-Y_2O_3, $YMnO_3$ and $Y_2Cu_2O_5$, along with a perovskite phase. DC electrical conductivity measurements have shown a semiconducting behaviour for all the solid solutions with perovskite-type structure. The room temperature conductivity increases with Cu until ~33 at.% Cu, and then decreases. Thermally activated small polaron hopping mechanism, between Mn^{3+} and Mn^{4+} cations, controls the conductivity in these ceramics. Results are discussed as a function of the Mn^{3+}/Mn^{4+} ratio for each composition. © 2002 Published by Elsevier Science Ltd.

Keywords: Electrical properties; Manganites; Perovskites; $(YCu_xMn)O_3$; Electrical conductivity

1. Introduction

The rare earth (RE) manganites have been the focus of much interest because of their electrical and magnetic properties such as its semiconducting behaviour and magnetoresistive features. Much work have been devoted to the research of the properties of light RE manganites, particularly to the knowledge of the features of the $LaMnO_3$ compound modified when Ba, Sr, or Ca substitutes for La.[1,2] Use of these solid solutions as ceramic electrodes for solid oxide fuel cells (SOFCs) has been studied for several years.[3,4] More recently, the colossal magnetoresistive effect found in both single crystals and ceramic bodies of those solid solutions have been extensively treated by many authors.[5]

The light RE manganites crystallise with a perovskite-type structure and Space Group Pbnm, which tends to increase its anisotropy when the atomic weight of the RE rises, and their ionic radii decrease, from rhombohedral, quasi-cubic symmetry for La, to orthorhombic symmetry, for Dy manganite with high b/a ratio. From the Er manganite, including the Y manganite, the RE manganites crystallise with a hexagonal symmetry and Space Group $P6_3cm$ [6] in spite of the respective values of the Goldschmidt tolerance factor, $\mathbf{t}=(r_A+r_O)/(r_B+r_O)^*\sqrt{2}$, for the perovskite-type structure. The structural change from perovskite-type to hexagonal symmetry can be associated, not only to the decrease of the tolerance factor, but also to the presence of a Jahn-Teller-type Mn^{3+} cation on B sites with octahedral coordination. Such a cation promotes a strong anisotropic co-operative deformation, which induces the change of symmetry when the tolerance factor attains a small enough value.[7] On the contrary, the heavy RE ferrites, such as the $ErFeO_3$ with the same tolerance factor, ~0.80, of $ErMnO_3$, crystallises with an orthorhombic perovskite-type structure.

$YMnO_3$ is a ferroelectric, antiferromagnetic compound with a very low value of electrical conductivity.[8] At high voltages it shows a peculiar non-ohmic behaviour.[9] The solid solutions with the $CaMnO_3$ perovskite structure showed a transition to this $CaMnO_3$ structure for an amount of approximately 22 at.% Ca.[10] Similar behaviour was noticed when the Ni cation[11] or Co

* Corresponding author. Tel.: +34-918-711-800; fax: +34-918-700-550.
E-mail address: cmoure@icv.csic.es (C. Moure).

0955-2219/02/$ - see front matter © 2002 Published by Elsevier Science Ltd.
PII: S0955-2219(02)00050-X

cation[12] substitute for Mn cations. In this case, ~20 at.% Ni is enough to change the structure from hexagonal, $YMnO_3$-type to perovskite-type structure, whereas ~25 at.% of Co are necessary to cause the same change. A solid solution limit has been established for Ni amount higher than 50 at.%. On the other hand, the Co-containing solid solution is extended at least up to 70 at.% Co. Both of these solid solution types are semiconducting compounds, with a small polaron hopping thermally activated as conductivity mechanism.

Both cations are divalent, although Co may also adopt a trivalent state. Both show not Jahn-Teller behaviour. On the contrary, Cu^{2+} is a divalent stable cation with d^9 configuration, which makes it to be a Jahn-Teller cation, such as Mn^{3+}.

The scope of this work is to study the effect of the incorporation of the Cu^{2+} cation on the structure, symmetry and electrical properties of the $Y(Cu,Mn)O_3$ solid solution and to compare with that observed on parent systems $Y(Ni,Mn)O_3$ and $Y(Co,Mn)O_3$.

2. Experimental methods

$Y(Cu_xMn_{1-x})O_3$ compositions with $x=0.20$–0.60 were prepared by solid state reaction of stoichiometric mixtures of reagent grade MnO, CuO and Y_2O_3 (Aldrich, Chemical Co. Inc., Milwaukee, WI), with submicronic particle size. The mixtures were homogenised by wet attrition milling using isopropanol as liquid medium. The dried mixtures were calcined at 1000 °C for 1 h. The calcined cakes were remilled by the same technique, dried, granulated and uniaxially pressed. Granulometric analysis was carried out on the synthesised powders by means of laser counting, (Mastersizer model, Malvern Instruments, Ltd, UK) and BET techniques, (Quantachrome MS-16 model, Syosset, NY). Pressed pellets were sintered in air between 1100 and 1325 °C for several cycles. Apparent density was measured by water displacement. X-ray diffraction (XRD) analysis was performed both on the calcined powder and on the sintered samples using a D-5000 Siemens Diffractometer and CuK_α radiation. The powder was identified by scanning at a rate of 2° 2θ/min, and the lattice parameters were calculated from the spectra obtained on the sintered samples at a scanning rate of 0.5° 2θ/min. Si powder was employed as an internal standard. The microstructure of the sintered ceramics was observed by scanning electron microscopy (SEM), (Zeiss DSM 950, Oberkochem, Germany) on polished and thermally etched surfaces. The thermal etching was carried out at a temperature which was 90% sintering. Bars-shaped samples were painted with silver paste and fired at 775 °C for 1 h. Four-point DC conductivity measurements were carried out for all the solid solutions with perovskite-type structure between 25 and 700 °C. For the measurements, a Constant Current DC power supply (Tektronix, model PS280) and a HP Multimeter (model 44201A), with 1 μA DC current resolution were used. Activation energies were calculated from the corresponding Arrhenius plots.

The Seebeck-Coefficient measurements were made on cylindrical samples, 0.3 cm in diameter and 1.5 cm long, using a quasi-conventional technique for a rapid and qualitative determination of the majority charge-carrier sign.[13] For the measurements, two metal blocks containing the thermocouples held the sample. A heater on one block produced the temperature gradient in the sample. The thermoelectric voltage was measured between the same reference points.

The Goldschmidt tolerance factor, **t**, has been calculated using the ionic radii tabulated by Shannon,[14] taking into account the oxygen co-ordination number of cations and the existence of different valence states of the Mn and Cu cations, with different ionic radii, in the solid solutions. Mean ionic radius on B lattice sites has been used when two or more cations are present on that site.

3. Results

The apparent particle size, as measured by laser counting, was 1.3 μm, but this size corresponds to that of aggregates. The BET measurements indicated specific surface area values of 5 m^2/g, which correlates well with an average particle size of ~0.20 μm.

Table 1 summarises some results of the relative density of sintered ceramics. The relative values have been referred to the theoretical density, D_{th} that has been calculated from the measured lattice parameters, using the chemical formulae $Y(Cu_xMn_{1-x})O_3$ for the different x values. Possible deviations on the oxygen stoichiometry have not been taken into account for this calculation. It can be seen that the density values always were in the 95–97% D_{th} range for sintering temperatures of 1150 °C. Sintering at higher temperatures led to a lowering of the apparent density. It is possible that a desintering process takes place, with pore coalescence and growth.

Fig. 1 shows the microstructure of the 33/67 sample, on the polished surface, (A), and on the fresh fracture

Table 1
Relative density of ceramics sintered in air at several temperatures

At.% Cu	D_r (%) 1150 °C —2 h	D_r (%) 1325 °C —2 h
30	96.9	89.1
33	96.4	86.2
40	96.1	85.2
45	95.2	89.1
50	95.4	90.2

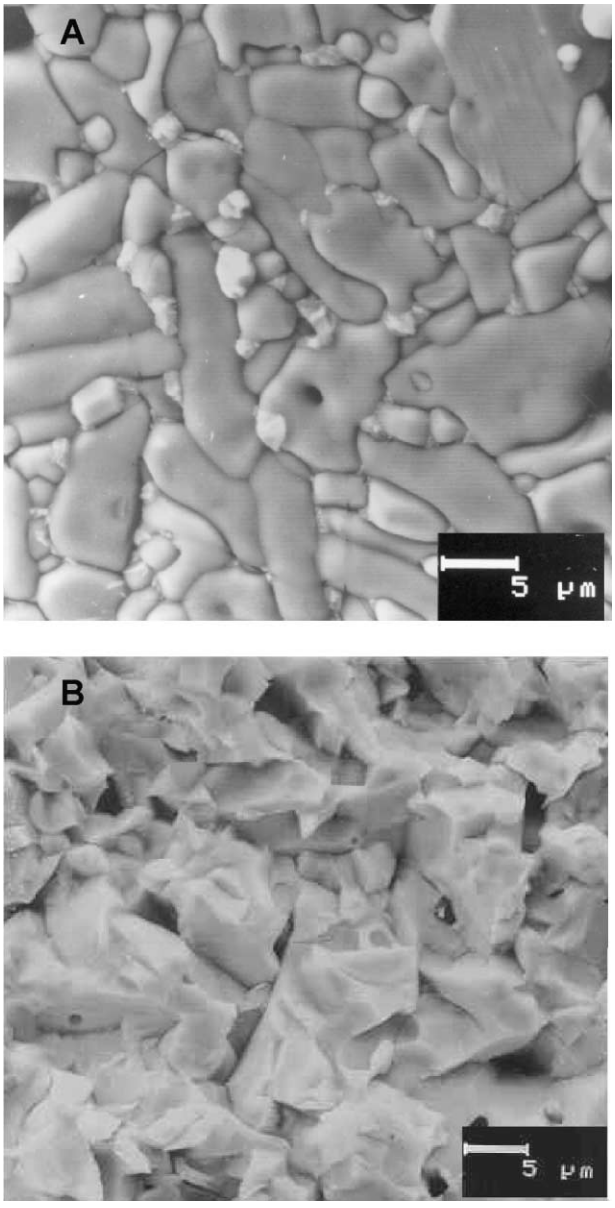

Fig. 1. Micrograph of polished and thermally etched surface (A), and fresh fracture surface (B) of a sintered sample corresponding to the composition with 33 at.% Cu, sintered at 1150 °C, 2h.

surface, (B). The microstructure is bimodal, with large and small grains, all of them in the microscale size range. The porosity is relatively low in concordance with the measured relative density. It can appreciate the existence of very rounded grains and small exsolutions in the grain boundaries. This seems to indicate that a small amount of liquid phase has been formed during sintering. The low melting temperature of CuO may be the cause of the appearance of a such liquid phase.

Fig. 2 shows the XRD patterns of samples with $x=0.20$, 0.33, 0.40 and 0.60. The diagrams were indexed according to a perovskite-type unit cell, with space group Pbnm. As can be seen, perovskite phase has been formed in all cases, including that corresponding to

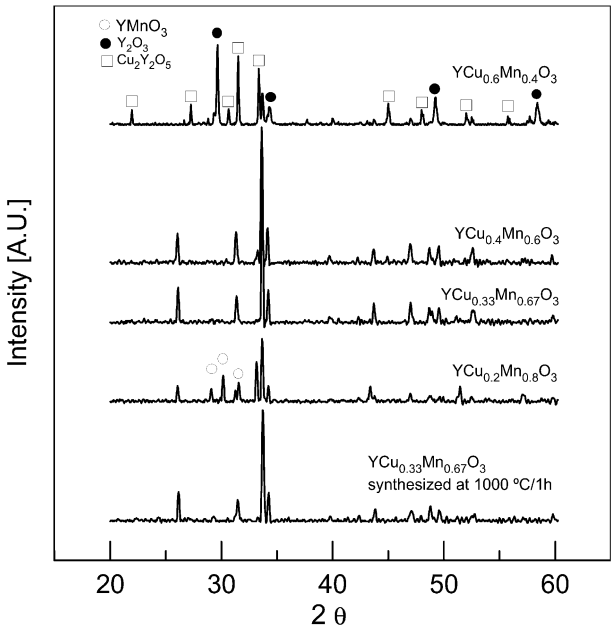

Fig. 2. XRD patterns of the solid solutions corresponding to samples with 20, 33, 40 and 60 at.% Cu sintered at 1150 °C.

$x=0.20$ and $x=0.60$. For $x=0.2$, some amount of pure $YMnO_3$ is still present. On the other hand, samples with $x>0.50$ also showed presence of Y_2O_3 and of $Y_2Cu_2O_5$. Only in the $0.30\leqslant x\leqslant 0.50$ range was it possible to appreciate existence of a pure perovskite-type phase.

Table 2 shows the measured lattice parameters of the solid solutions, including orthorhombicity factor, b/a, and cell volume. The incorporation of Cu cations causes only a small decrease of the b parameter, and a slight decrease of the a parameter. As consequence, the orthorhombicity parameter b/a is maintained almost constant. There is also a smooth decrease of the lattice volume, i.e. the compactness grade of the perovskite lattice rises slightly. The perovskite lattice shows, in all the samples corresponding to the earlier mentioned existence range, a lattice parameter relation $c/\sqrt{2}<a<b$, such as is seen in Fig. 3. Therefore, the perovskite lattice is of O′-type orthorhombic structure.[15]

Fig. 4 shows the evolution of the tolerance factor, **t**, against the Cu amount. For comparison, the evolution of **t** in the systems $Y(Ni,Mn)O_3$ and $Y(Co,Mn)O_3$ are also represented.

Fig. 5 depicts the σT against $1/T$ curves for single-phase compositions with perovskite-type structure. Table 3 shows the room temperature conductivity and the activation energy of all the samples. According to the obtained results, the conduction mechanism is via thermally activated small polaron hopping. Fig. 5 also shows the existence of a maximum in the conductivity for the 33/67 Cu/Mn ratio sample. From this ratio, the conductivity decreases up to the cation ratio of 50/50. The electrical conductivity behaviour is such as is typi-

Table 2
Lattice parameters of the solid solution $Y(Cu_xMn_{1-x})O_3$

At.% Cu	20[a]	30	33	40	45	50
a, (nm)($\pm$0.0001)	0.5246	0.5253	0.52555	0.5247	0.5247	0.5246
b($\pm$0.0001)	0.5730	0.5719	0.5715	0.5718	0.5714	0.5722
c($\pm$0.0001)	0.7382	0.7363	0.7362	0.7367	0.7371	0.7368
b/a	1.092	1.089	1.088	1.090	1.089	1.091
V (nm^3)($\pm$0.0004)	0.2219	0.2212	0.2211	0.2211	0.2210	0.2212

[a] Biphasic region.

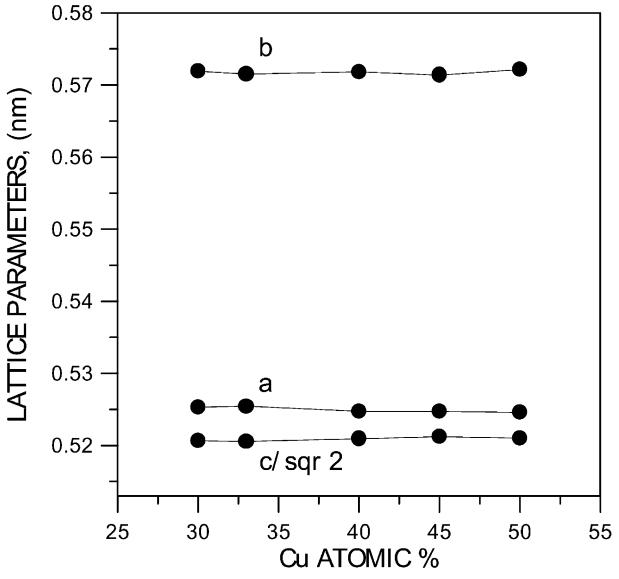

Fig. 3. Variation of lattice parameters against Cu content in the compositional range of pure perovskite. $c/\sqrt{2}$ has been represented instead of c, for visualizing the O′-type structure nature.

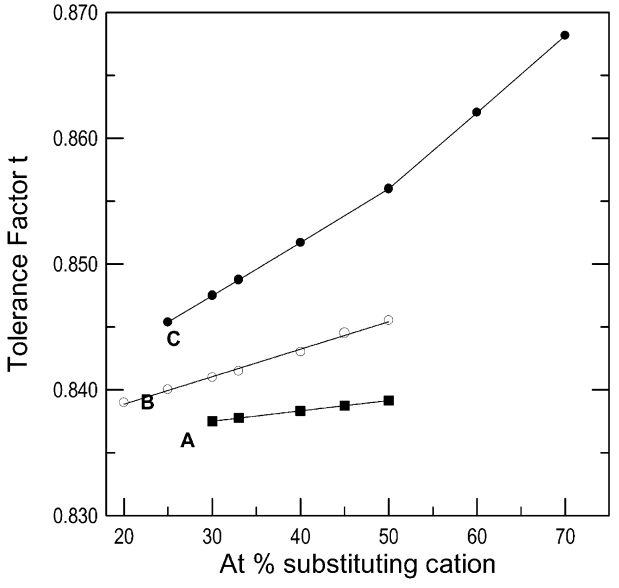

Fig. 4. Variation of tolerance factor **t** against substituting cation for (A) $YCu_xMn_{1-x}O_3$ solid solution; (B) $YNi_xMn_{1-x}O_3$ solid solution; and (C) $YCo_xMn_{1-x}O_3$ solid solution, (the last two have been taken from Refs. 11 and 12, respectively).

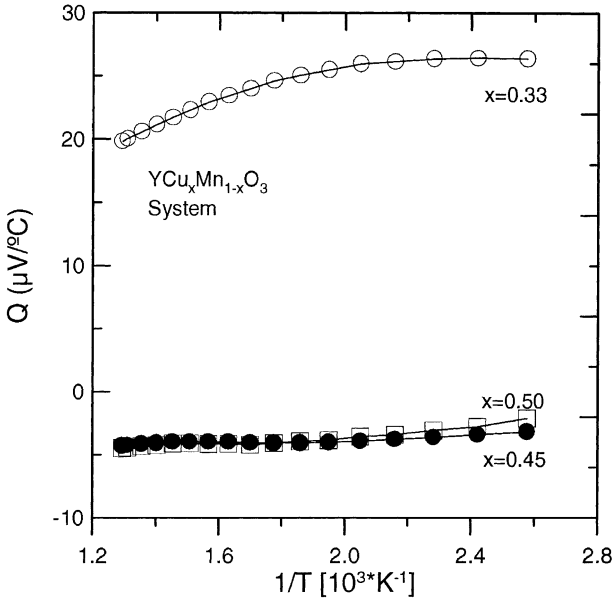

Fig. 5. Log σT vs $1/T$ for different compositions.

Table 3
Electrical conductivity at 25 °C and activation energy for the perovskite solid solution as a function of the Co amount

At.% Cu	30	33	40	45	50
$\sigma_{25^\circ C}$ (S m^{-1})	0.133	0.232	0.079	0.092	0.070
E_{ac} (eV)	0.26	0.24	0.27	0.29	0.26

cally described for the manganites with perovskite-type structure.[16]

Fig. 6 shows the Seebeck-Coefficient of the different solid solutions with perovskite-type structure. Measured values correlate well with the proposed semiconduction mechanism of small polaron hopping. Typical values of 20 μV/°C have been determined. It is possible to see that the sign of charge carriers changes when the Cu amount is higher than 33 at.%, such as was observed in the $Y(Ni,Mn)O_3$ system.[11]

4. Discussion

The crystal-chemical behaviour of the samples containing $\geqslant$50 at.% Cu differs to that observed in the parent systems $Y(Ni,Mn)O_3$ [11] and $Y(Co,Mn)O_3$.[12] The progressive substitution of the Jahn-Teller cations, Mn^{3+} for other Jahn-Teller cations, with (II) valence value induces the formation of Mn^{4+} to preserve the valence equilibrium, but the lowering of the presence of Jahn-Teller cations in the lattice by the change of Mn^{3+} to Mn^{4+} is lesser than that produced by the incorporation of a non-Jahn-Teller cation, such as Ni^{2+}, because each substituted Mn^{3+} is replaced by a new Jahn-Teller

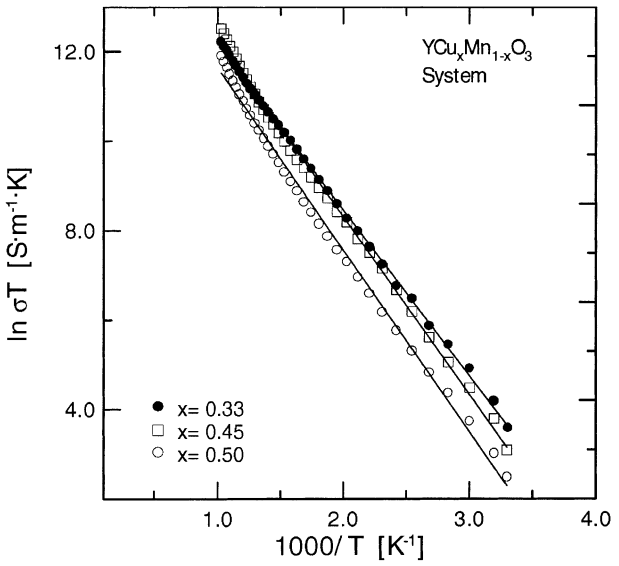

Fig. 6. Seebeck-Coefficient vs. temperature for different solid solutions with perovskite-type structure.

cation, Cu^{2+}. Nevertheless, the high anisotropy of the crystalline lattice decreases slightly, and this decrease is enough to promote the appearance of a perovskite-type phase. When the Cu-containing system is compared with the Ni-containing one, it can be seen that the amount of modifying cation necessary to attain a single phase, with perovskite-type structure, is higher for the Cu cation. The reason can be related to the earlier point: at low ratios of substituting Cu^{2+} cation, a significative amount of Jahn-Teller anisotropic cations are maintained in the lattice of the solid solutions. As consequence, the amount of Mn^{3+}, which must be transformed to Mn^{4+} to attain an adequate ratio between Jahn-Teller and non-Jahn-Teller cations to induce a phase transition, would be higher than that which is needed to produce the same effect in the $Y(Ni,Mn)O_3$ and $Y(Co,Mn)O_3$ systems.

The O′-type orthorhombic perovskite shown by the solid solution in the compositional range for which it exists pure perovskite phase, corroborates the effect produced by the presence of substituting Jahn-Teller on the perovskite lattice. In the Ni- and Co-containing solid solution with the same compositional substitution, it has been stated that the perovskite crystallised as an O-type orthorhombic structure. This type of structure corresponds to those compositions with a higher degree of symmetry, i.e. less distorted structure.[15] Besides that, the Cu-containing solid solution showed the lower tolerance factors with regard to the other two systems, with a very small variation against the x value. This low value of **t** agrees well with the strongly distorted nature of the corresponding perovskite structure.

On the other hand, there is a similitude of the present system with regard to the $Y(Ni,Mn)O_3$ one. The obtained results seem to indicate that the Cu cannot take a valence state of 3+, i.e. it seems to be non-feasible to form a perovskite structure with the following ion distribution:

$$Y\left[Cu^{2+}_{0.40}Mn^{4+}_{0.40}Cu^{3+}_{0.20}\right]O_3,$$

therefore, the 50/50 composition is the boundary between a monophasic field and a new multiphase field.

The conductivity behaviour correlates well with the crystalline results. The progressive substitution of Cu^{2+} for Mn^{3+} cations leads to an initial increase of the Mn^{3+}–Mn^{4+} localised states, until $x=0.33$, followed for a decrease when $x>0.33$, for which the Mn^{3+} decreases rapidly. The model is similar to that applied in the Ni-containing system to explain the same behaviour.[11] According to this model, the Cu^{2+} would not contribute to the conduction mechanism, because of the lack of another valence state of Cu in the nearest neighbour sites. The only pair contributing to a controlled valence mechanism would be the Mn^{3+}–Mn^{4+} pair. If it is supposed to be a complete valence compensation, it is easy to see that the number of these possible pairs increases up to a 33/67 Cu/Mn content ratio. A subsequent rise in the Cu percentage leads to a decrease in the concentration of possible forming pairs. It is possible to form 0.33 pairs per formula unit in the 33/67 compositions, whereas it is possible to form only 0.2 in the 40/60 composition, and 0.1 in the 45/55 one. This variation in the relative percentage between the two possible Mn cations explains the existence of a maximum in the conductivity values at an intermediate value of x, and the subsequent decrease up to 50 at.% Cu percentage.

Measured values of the Seebeck-Coefficients of the solid solution, as shown in Fig. 6, seem to corroborate the crystalline model established earlier. It is possible to see that the sign of charge carriers changes when the Cu amount is higher than 33 at.%. This fact corroborates the earlier statement about the contribution of only Mn^{3+}–Mn^{4+} pairs to a semiconducting mechanism. The samples with $Cu\leqslant 0.33$ have a percentage of Mn^{3+} higher than that of Mn^{4+}. Therefore, the predominant charge carriers are holes. For $Cu\geqslant 0.33$, Mn^{4+} is higher than the Mn^{3+} amount. As consequence, the predominant carriers must be electrons.

5. Conclusions

The substitution of Cu^{2+} for Mn^{3+} in the hexagonal $YMnO_3$ compound leads to a phase transition from hexagonal phase to an O′-type orthorhombic perovskite phase for Cu amounts ~30 at.%. The reason for this transition is related to the decrease of the Mn^{3+} Jahn-Teller cation concentration in the lattice. The Jahn-Teller nature of the Cu^{2+} is, probably, the cause of the

displacement towards higher contents of the modifying cation the limit from which the phase transition takes place. Above 50 at.% Cu, a multiphase system is developed, in which a perovskite-type phase co-exists with $YMnO_3$, $Y_2Cu_2O_5$ and Y_2O_3 phases, indicating the high stability of the Cu(II) valence state.

The perovskite-type solid solutions, ($x = 0.30$–0.50) are semiconducting materials. The conduction mechanism is via thermally activated small polaron hopping. A change in the sign of the charge carriers, from holes to electrons is observed at the 33/67 Cu/Mn ratio.

Acknowledgements

This work was supported by Spain CICYT-MAT-2000–0815

References

1. Misuzaki, J., Tagawa, H., Naraya, K. and Sasamoto, T., Non-stoichiometry and thermochemical stability of the perovskite-type $La_{1-x}Sr_xMnO_{3-\delta}$. *Solid State Ionics*, 1991, **49**, 111–118.
2. Li, Y. H., Damay, F., Cohen, L. F., Thomas, K.A, Hossain, A. K. M. and MacManus-Driscoll, J. L., Structure and magnetic properties of $La_{0.7}Ca_{0.3}MnO_{3-\delta}$ for $(3-\delta) < 3.0$. *J. Am. Ceram. Soc*., 2001, **84**, 747–752.
3. Ostergard, M. J. L. and Mogensen, M., AC impedance study of the oxygen reduction mechanism on $La_xSr_{1-x}MnO_3$ in SOFC. *Electrochimica Acta*, 1993, **38**, 2015–2020.
4. Hammouche, A., Siebert, E. and Hammou, A., Crystallographic, thermal and electrochemical properties of the system $La_{1-x}Sr_xMnO_3$ for high temperature solid oxide fuel cells. *Mater. Res. Bull*., 1989, **24**, 367–80.
5. Urishabara, A., Moritomo, Y., Arima, T., Asatmisu, A., Kido, G. and Yokura, Y., Insulator-metal transition and giant magnetoresistance in $La_{1-x}Sr_xMnO_3$. *Phys. Rew. B*, 1995-II, 51, **14**, 103–109.
6. Muller, O. and Roy, R., *The Major Ternary Structural Families*. Springer Verlag, New York, USA, 1974.
7. Yakel, H. L., Koehler, W. C., Bertaut, E. F. and Forrat, E. F., On the crystal structure of the manganese(III) trioxides of the heavy lanthanides and yttrium. *Acta Cryst*, 1963, **16**, 957–962.
8. Coure, Ph., Guinet, Ph., Peuzin, J., Buisson, G. and Bertaut, E. F., Ferroelectric properties of hexagonal orthomanganites of yttrium and rare earths. *Proc. Int. Meeting Ferroelectricity*, 1966, **V**, 332–340.
9. Moure, C., Fernandez, J. F., Villegas, M. and Duran, P., Non-ohmic behaviour and switching phenomena in $YMnO_3$- based ceramic materials. *J. Eur. Ceram. Soc*., 1999, **19**, 131–137.
10. Moure, C., Fernandez, J. F., Villegas, M., Tartaj, J. M. and Duran, P., Phase transition and electrical conductivity in the system $YMnO_3$–$CaMnO_3$. *J. Mater. Sci*., 1999, **34**, 2565–2568.
11. Gutierrez, D., Peña, O., Duran, P. and Moure, C. Crystal structure, electrical conductivity and Seebeck coefficient of $Y(Ni,Mn)O_3$ solid solution. *J. European Ceram. Soc*., 2002, **22**, 567–572.
12. Gutierrez, D., Peña, O., Duran, P. and Moure, C. Crystalline structure and electrical properties of solid solution $Y(Co,Mn)O_3$, Presented at the V National Meeting on Electroceramics, Barcelona, (Spain), 30 May–1 June 2001. *J. Euro. Ceram. Soc*. (submitted for publication).
13. Heikes, R. and Ure, R., *Thermoelectricity: Science and Engineering*. Interscience Publishers, New York, 1961.
14. Shannon, R. D., Revised effective ionic radii and systematic studies of interatomic distanced in halides and chalcogenides. *Acta Cryst*., 1976, **A32**, 751–767.
15. Pollert, E., Kupricka, S. and Kuzmisova, E., Structural study of $Pr_{1-x}Ca_xMnO_3$ and $Y_{1-x}Ca_xMnO_3$. *J. Phys. Chem. Solids*, 1982, **43**, 1137.
16. Subba Rao, G. V., Wanklyn, B. M. and Rao, C. N. R., Electrical transport in rare-earth ortho-chromites,-manganites and ferrites. *J. Phys. Chem. Solids*, 1971, **32**, 345–358.